University of Huddersfield Repository

Xu, Qihua, Xu, Qiang and Lu, Zhongyu

The development of creep damage constitutive equations for low Cr-Mo alloy steel and its weldment at low stress

Original Citation

Xu, Qihua, Xu, Qiang and Lu, Zhongyu (2013) The development of creep damage constitutive equations for low Cr-Mo alloy steel and its weldment at low stress. In: 6th International 'HIDA' Conference: Life/Defect Assessment & Failures in High Temperature Plant, 2nd-4th December 2013, Nagasaki, Japan.

This version is available at https://eprints.hud.ac.uk/id/eprint/23246/

The development of creep damage constitutive equations for low Cr-Mo alloy steel and its weldment at low stress

Qihua Xu[1], Qiang Xu[2], Zhongyu Lu[3]
School of Computing and Engineering, University of Huddersfield, Huddersfield, HD1 3DH, UK
[1]U1372662@hud.ac.uk; [2]Q.Xu2@hud.ac.uk; [3]Z.Lu@hud.ac.uk

Corresponding author: Qiang Xu, Q.Xu2@hud.ac.uk

Abstract: The ultimate objective of this research project is to develop creep damage constitutive equations for low Cr-Mo alloy and its weldment under low stress (0.2-0.4 yield stress, σ_Y). This paper summarizes a critical analysis on the cavity nucleation and growth and the deformation mechanisms and creep damage evolution characteristics at low stress with temperature ranging from 450 °C to 650 °C, in order to firmly establish the physical base for the theoretical constitutive modeling work. Moreover, it covers the influence of the stress level on the development of cavity nucleation and growth, leading to the final rupture, and proposes and discusses a new idea for failure criterion to be used in the constitutive equations under uni-axial stress state. This paper contributes to knowledge and the development of methodology.

Key words: cavitation; creep damage; low stress; grain boundary fraction

1. Introduction

Low Cr-Mo alloy steel is widely used for steam pipeworks in the power generation industry, particularly in fossil fuel plants and nuclear reactors at elevated temperatures of 450-550 $°C$ and with stress levels of 40-200 MPa. This steel is selected as it offers the necessary creep strength at optimal cost. In attempt to expand its application, experimental work has been carried out to a wider range of stress (30-350 MPa) and even higher temperature (up to 650 $°C$) [1]. This results in the need to understand and monitor the creep deformation and damage evolution under the lower stress level. The long life of power generation installation signifies the importance of lifetime prediction under low stress. That is the concern of this research project. Here, a stress level is conventionally deemed as low, intermediate, or high, depending on its ratio to the yield stress ($0.2\text{-}0.4\sigma_Y$, $0.4\text{-}0.5\sigma_Y$, and $> 0.5\sigma_Y$, respectively) at a particular temperature.

Most frequently applying temperature and the average operating stresses for low Cr-Mo alloy, such as, 0.5Cr0.5Mo0.25V, 0.5CrMoV, 1CrMoV,1.25Cr-1Mo and 2.25Cr-Mo alloy, is approximately 450~600$°C$ at approximately of 50~100MPa, within low stress level ($0.2\sigma_Y\text{-}0.4\sigma_Y$). Clearly evidences from the industry and research institutions show the need for a new set of creep damage constitutive equations which is capable to depict the creep deformation, damage, and rupture under low stress level accurately [2-4].

The most popular Kachanov-Robatnov-Hayhurst (KRH) creep damage constitutive equations formulation was not necessarily developed and calibrated for low stress level and cannot depict the creep strain accurately under multi-axial state of stress due to its three-dimensional generation method used [4-6]. In 2004, the ECCC (European Creep Collaborative Committee) [2] established a new project to develop a new set of constitutive equations for low alloy steel because the previous creep model cannot present accurate results for the high temperature industry. Likewise, the same requirement raised by ECCC was raised by the Nuclear Research Index (UK) [3] to ensure the inspection of operated components. In 2012, Hosseini et al. [7] of the SFL (Swiss Federal Laboratories) demonstrated that the lifetime for lower stress is overestimated by the five different sets of creep models found from literature; moreover, these creep models do not depict the tertiary stage which is closely related with lifetime fracture [7]. Therefore, it is important to conduct a critical review on the creep deformation process and rupture mechanisms to firmly establish the foundation for the constitutive modelling work. At this current stage, the authors believe that for low alloy Cr-Mo steel there is a lack of clarity of the creep damage processes at different stress levels and stress states, as well as a lack of good understanding of the microstructure changes, particularly on the cavitation, during creep services for constitutive modelling work.

This paper is an expanded version of the authors' previous published work on a critical analysis of creep deformation and rupture under different stress level at various constant temperature of the low Cr-Mo alloy, such as 2.25Cr-1Mo (T/P22) steel [8-10]. It contains further detailed analysis of cavity nucleation and growth experimental data, and the new failure criterion. The paper is organized as follows: Section 1 presents the introduction; Section 2 summarises the effect of stress level on lifetime, minimum creep strain rate, et al; Section 3 reports on an analysis of cavitation characteristics (such as typical cavity site, cavity shape, cavity nucleation density and rate, and cavity growth size and rate during its lifetime for low Cr-Mo alloy steel and its weldment, especially on Type IV failure) and the typical cavity nucleation and growth mechanisms; Section 4 discusses the existing creep rupture criteria used for uni-axial specimens, and the proposal of grain boundary fraction area and the coupling of the micro-damage and macro creep deformation; Section 5 presents the summary of the preliminary results and discussions, as well as the key requirements for developing the new set of creep damage constitutive equations; and Section 7 draws the conclusion and raises the further work.

2. Effect of Stress Level under Uni-axial Creep

The creep data to be analyzed for the creep damage and rupture processes were extracted from published literatures and research institutions' laboratories (universities, companies and high temperature industries) [1, 11-14].

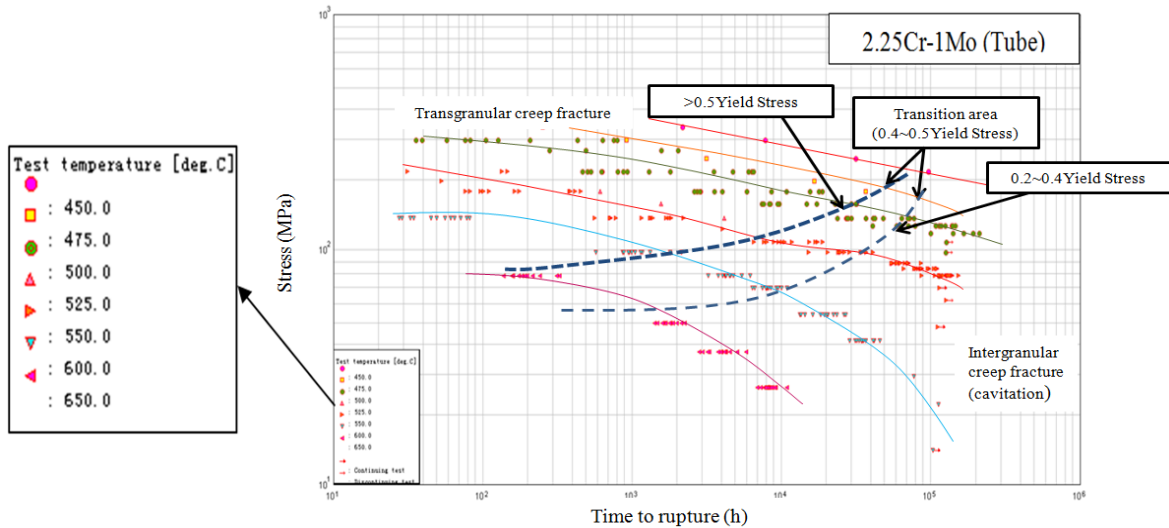2.1. Effect of the stress level on creep lifetime

Fig. 1 Stress versus time to for T22 steel (tubes) [1]

Figure 1 clearly demonstrates the effect of stress level on the lifetime for the range of temperature tested (450 °C to 650 °C) Figure 1 also reflects that at higher stress levels the damage mechanism differs from the low stress levels. This observation firmly indicates that extrapolation from short-term (high stress level, $\geq 0.5\sigma_Y$) data to long-term (lower stress, $0.2\sigma_Y \sim 0.4\sigma_Y$) is highly questionable, no matter how convenient and attempting it is; a specific creep damage constitutive equation has to be developed according to the stress level in order to reflect the changing of damage mechanisms. This is also in agreement with the general observation of stress breakdown in creep modeling for other materials.

Based on the experimental data of the stress versus time to the rupture, the mechanical relationship could be approximately assumed as:

$$T_f \propto \frac{1}{\sigma} \qquad (1)$$

where T_f is rupture time, and σ is external applied stress.

2.2. Effect of the stress level on minimum creep rate [1, 11-13]

In view of the importance to obtain the relationship between the applied stress and the minimum creep rate, an analysis has been carried out on experimental data with a range of stress and temperature [1, 11-13].
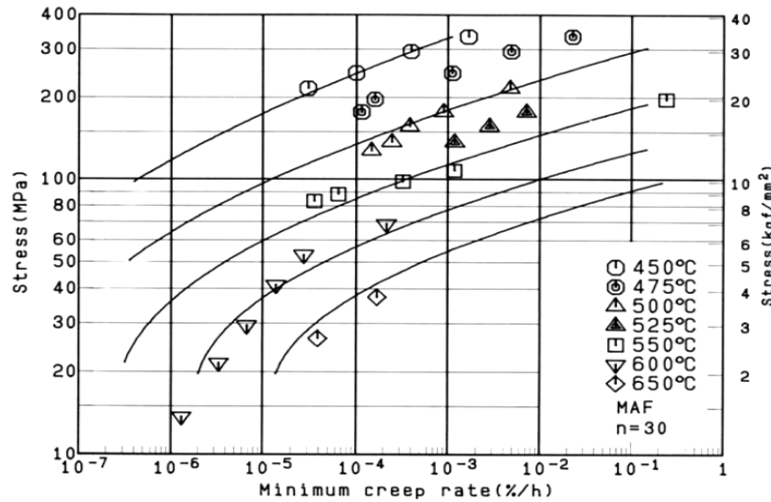
Fig. 2 The stress versus minimum creep rate relation for P22 steel (tubes) [13].

Figure 2 shows the effect of stress level on minimum creep rate of the alloy 2.25Cr-1Mo at the temperature range of 450℃-650℃ and stress range of $10MPa$~$400MPa$ [13].

Using the experimental data tested at 600℃ within the low stress level as the representative one for low stress level, it shows approximately a linear relation between the minimum creep strain rate and stress in log-log scale, it reveals that the power law may still applies under low stress level.

$$log\dot{\varepsilon}_{min} \propto n * log\sigma \qquad (2)$$

where, $\dot{\varepsilon}_{min}$ is minimum creep rate, σ is external stress. The value for n was found as 5.34x10^{-6} (MPa^{-1}) for the above specific temperature.

From the above Fig. 2, it can also be seen that the gradient of the stress and minimum creep strain for intermediate and/or high stress levels increases.

3. **Cavitation Characteristics** [15-29]

In order to obtain a precise understanding of the creep damage and rupture process, a critical analysis on the micro-structural changes and the cavity nucleation, growth and coalescence process under different stress levels was carried out and the results are presented below. It is well known that the final rupture life of such material operated at elevated temperature has been influenced by both of the micro-structural changes and development of cavities, however, large amount of experiments indicate that the dominant accumulated damage is caused by cavity development [15-29].

3.1. Creep cavity site and cavity shape [15-29]

Under low stress, the distribution of the cavity was observed perpendicular (90°) to the external applied stress [15]; this has been confirmed in [16-21], which claimed that with a low applied uniaxial stress (50-80MPa) specimens failure is resulted from the coalescence of discrete cavities on prior austenite grain boundaries which were oriented approximately to the tensile stress axis. Moreover, Kawashima stated that the cavity has also been seen at 45° to the tension stress [20]. The creep cavities have been observed to nucleate at carbides, second phase particles, a ridge, a triple point and inclusions along the grain boundaries [21]. For instance, the sulphide particles which are the primary nucleation sites in the overheated condition tend to nucleate cavities early in creep life [15-21]. The reports from EPRI indicated that the cavity preferred to nucleate at stress concentration point on grain boundaries under low stress level [22].

Table 1 Effect of stress level and initial creep cavity shape [15-21].

Stress level	Low stress (0.2~$0.4\sigma_Y$)	High stress (0.2~$0.4\sigma_Y$)
Typical cavity shape	Spherical voids	Circular voids

As Table 1 shows the typical initial creep cavity shape under different stress levels; the observation from literatures experiments found that at lower stresses, the shape of the cavity is spherical [15-24]; for the higher stress regime, the cavity shape normally presents as circular during most of the secondary creep stage [15-24] due to the influence of local stress concentration.

3.2. The cavity nucleation and growth behavior under low stress level

The nucleation and growth of cavities process has been investigated from the literature [15-25]. At low stress, （$0.2\sim0.4\sigma_Y$） the nucleation controlled constrained cavity growth is predominant mechanism [21-29]; furthermore, fracture behavior has been observed as intergranular rupture along the grain boundaries [15-28]; further analysis illustrates the creep failure is associated with brittle rupture behavior as the reduction of area is approximately less than 10% [1, 11-14, 21-28].

Fig. 3 summarized the observation of cavitation which were reported in [15] by Dobrazanski and et al. for 1Cr-0.5Mo alloy steel at 520-560℃ with low stress of 35-120MPa. These observations have been applied against the trend of typical creep stages by the authors, indicating the internal creep damage processes in low Cr-Mo alloy with time to fracture. Dobrazanski and his fellows [15-18] stated that for the creep evolution of low-alloy Cr-Mo steel, in the early stages (≤ less than and equal to 0.4 of time to rupture T/T_f) of creep damge development, individual voids are observed (at stage 1 in Fig. 1). His research reflects that under low stress level, for the 1Cr-0.5Mo, T/P23 and P92 steel start to nuclei at about 0.4~0.6 T_f [15-18]. Similar initial development of cavitation nucleation process has been seen at approximately 0.25 T_f in the report form EPRI for 2.25Cr-1Mo steel of its creep fatigue specimens [30]. As further damage accumulates, the density of voids increases and the voids increases in size (at stage 2)[21-29]. Eventually, the density of voids is sufficient for cracks to form [21-29].
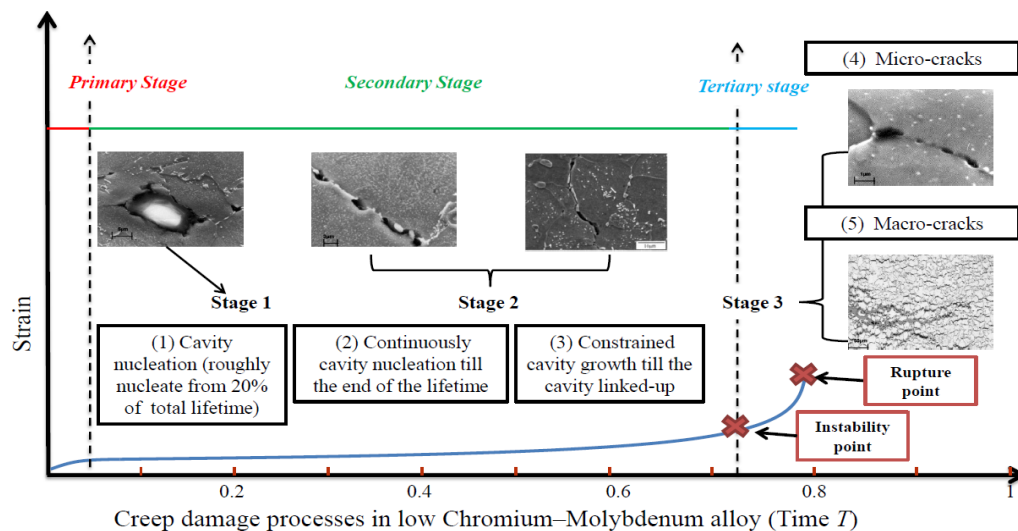

Fig. 3 Typical damage micro-structural from [15] has been associated with the typical curve, reflecting the dominant creep damage processes (cavitation) with typical creep curve for low Cr-Mo alloy steel at lower stress (0.2~0.4 σ_Y).

Initiation behaviour about the development of cavity has included 5 different processes: cavity nucleation, growth, and coalesce, micro-cracks growth and macro-cracks growth processes; these five process has been summarized associated with time to rupture in Table 2; As Table 2 shows the majority of life span is involved with the cavity nucleation from about $0.2T_f$ to $0.7T_f$ (stage 1), which takes about more than 50% of the total lifetime; nevertheless, the finial rupture process has only taken account about less than 30% of life to rupture (stage 3) [15-18], indicating that the assumption (all the void is nuclei at: $T_0 = 0$) is not suitable for low Cr-Mo alloy at lower stresses to develop a physical base set of creep damage constitutive equations.

Table 2 Initiation time for the development of cavitation process [15-18, 30]

Initiation behaviour at time to rupture: T/T_f	0-0.2	0.2-0.4	0.4-0.6	0.6-0.8	0.8-1
(1) cavity nucleation		≥0.25/0.26	0.4~0.6		
(2) cavity growth			0.38~0.56		
(3) cavity coalesce			≥0.4		
(4) micro-crack growth				≥0.78/0.85	
(5) macro-crack growth				≥0.7	0.96~1

Longsdale and Flewitt reported that under lower stresses (55.6, 60.6 and 70.6 *MPa*, at 600℃) for 2.25Cr-1Mo steel, the cavity nucleation rate of accumulation increases monotonically with time and at a given time was greatest for the largest applied stress [23, 25]; the density of the cavity observed on the grain surfaces increased continuously throughout the creep life [23, 25]; its cavity growth rate is slightly increased with the accumulation of time [23, 25].

All in all, under the low stress level, the failure is a brittle manner which was controlled by intergranular cavitation; the dominant process of creep damage accumulation which leads to eventually rupture is creep cavitation development, which is controlled by the continuous cavity nucleation and constrained cavity growth mechanism.

3.2.1. Cavity nucleation rate induced stress dependence under low stress level

Needham [21], by examine the smooth specimens, found the cavity nucleation rate strongly depends on the stress rather than on creep strain; the relative contributions of the principal, maximum and equivalent stresses to the creep on the nucleation rate, $\dot{N}$ and cavity growth rate, $\dot{R}$ in two Cr-Mo steels. He found that it is the principal tensile stress, σ_1, which controls the nucleation rate. He [21, 22] suggested that the functional relationship for cavity nucleation rate (Eq. 1), cavity growth rate (Eq. 2), and the rupture lifetime for 2.25Cr-1Mo steel and 1Cr-0.5Mo steel are inversely related to maximum principal stress, σ_1, by a power law, under lower stresses; the power law index number has been presented in Table 3 for these two Grades. Under low stress level, σ_1 controls the nucleation rate according to:
$$\dot{N} = \sigma_1^n \tag{3}$$
Under low stress level, σ_1 controls the nucleation growth rate according to:
$$\dot{R} = \sigma_1^m \tag{4}$$
Where n and m present as power law stress index summarised in Table 3.

Table 3 Summary of stress index for power law behavior under the low stress [21].

Under low stresses (0.2-0.4 Yield stress) *MPa*			
Depends on maximum principal stress	Cavity nucleation rate	Cavity growth rate	Rupture lifetime
Power law stress index(*n, m*)	5-7	3.5-4.5	4.8

This is simply illustrate that the influence of stress on cavity density, without reference to absolute cavity level. It is apparent that the relative cavity density is dependent upon the stress level. The proportionality of the cavity density to stress sometimes holds until very close to final failure [21-29]. This phenomenon shows the cavity nucleation occurs through out of the lifetime. The experimental observation shows that the continuous formation of cavities throughout life fraction is stress dependence [21-29].The predominance of the principal tensile stress was also found by Dyson and McLean [31] who carried out tests on Nimonic 80A in tension and torsion. The Von-mises stress, σ_e, is usually less important expect at high stresses in 2.25Cr-1Mo steel where Needham finds $\dot{N} \propto \sigma_1^4 \sigma_e^4$ [21].

3.2.2. Cavity density induced strain dependence under low stress level

As has been summarised in the previous section, it is agreed that cavity nucleation generally starts early and continues over an appreciable fracture of creep life. Quantitative measurements of the cavity nucleation rate have been made by counting the number densities of observable cavities at various fractions of the lifetime. These counts are usually made at cavity sizes of 0.5 to $1\mu m$, whereas cavity nuclei are much

smaller, say, 20nm.Therefore the apparent nucleation kinetics may be distorted by cavity growth. Dyson [21] , however, points out small cavities tend to grow rapidly and therefore the counting of cavities having a size of 0.5 μm reflects the kinetics of cavity nucleation sufficiently accurately in many practical cases.

Dyson [31] further noticed, a common result of many experimental studies is that the number of cavities, N, per unit grain boundary area increases approximately in proportion to creep strain with a factor of proportionality which, to a first approximation, is independent of stress. Likewise, Evans [24, 32] quotes a few other papers containing information on the increase in cavity number with strain. This observation can be expressed as:

$$N = \alpha' \varepsilon \tag{5}$$

where N is the cavities per unit grain boundary area α' is an empirical factor of proportionality having the physical dimensions [m^{-2}], and ε is creep strain; for austenized 2.25Cr-1Mo steel at 1300°C, $\alpha' = 4X10^{12}m^{-2}$; other low Cr-Mo alloy steel's empirical factor, such as, 1Cr1Mo0.25V steel austenized at 1300°C ($\alpha' = 4X10^{10}m^{-2}$) and 0.5Cr0.5Mo0.25V ($\alpha' = 1.5X10^{12}m^{-2}$) could be find in [24].

3.3. Cavity nucleation rate and cavity growth rates under high stress level

At high stress ($> 0.5 \sigma_Y$) , the plasticity-controlled cavity growth mechanism is predominant, and there is an increasing rupture strain with the increasing creep strain rate [15-18, 21-24, 33-34]. Under this stress level, the creep rupture occurs based on wedge-type micro-crack which formed at a triple grain junction and those cracks grow will lead to local grain-boundary separation [33-34]. Furthermore, failure occurs relatively quicker and is accompanied by elongation deformation, at this stress level [33-34]. The speed of plastic strain increasing rapidly after the external loading is applied. In this condition, the fracture is based on the transgranular cavities [33-35]. Further study shows the creep failure is associated with ductility because the specimens presented the reduction area is around ¾ of the cross section under high strength condition [35].

Creep deformation and rupture have been studied in 2.25Cr-1Mo steel over the range 100-210MPa (MN m^{-2}) at 565°C [21-28]. Kawashima and et al. reported that for this steel the creep ruptures lifetime dependences on the cavity nucleation rate and cavity growth size [20]. Creep damage accumulates by the initiation and growth of extensive cavitation at the prior austenite grain boundaries. Cavity formation predominates during the initial transient and individual cavities appear to nucleate on grain boundary carbides. Quantitative analysis of the cavitation kinetics in relation to the creep deformation processes suggests that cavity growth is directly related to deformation occurring at the grain boundaries. It is inferred that the cavity growth is limited by the local creep process occurring at the grain boundaries.

Table 4 The cavity growth rate versus stress in low Cr-Mo alloy, under high stress [20]

cavity growth rate(m/s)	stress (Mpa)
3.16228E-14	117.5
5.62341E-14	127.5
7.49894E-14	145
1.77828E-13	160
3.16228E-13	170
1.77828E-12	190
3.16228E-12	225

As Table 4 shows the growth rate increases with the increase of the applied stresses under higher stresses [20]. These results indicate that the cavity growth behavior is associated with the creep diffusion growth mechanism.3.3.1. Cavity nucleation rate induced stress dependence under high stress level

Under high stress level, Needham [21-22] claimed that the functional relationship for cavity nucleation rate, cavity growth rate, and the rupture lifetime for 2.25Cr-1Mo steel and 1Cr-0.5Mo steel are inversely related to maximum principal stress, σ_1, and and equivalent stress, σ_e, by a power law, under higher stresses; the power law index number is presented in Table 5 for these two grades.

Under low stress level, σ_1 and σ_e controls the nucleation rate according to:

$$\dot{N} = \sigma_1^a \sigma_e^b \tag{6}$$

Under low stress level, σ_1 and σ_e controls the nucleation growth rate according to:

$$\dot{R} = \sigma_1^a \sigma_e^b \tag{7}$$

where *a* and *b* present as power law stress index summarised in Table 5.

Table 5 Summary of stress index for power law behaviour the under high stress [21]

Under intermediate and high stresses (>0.5 Yield stress) MPa			
depends on maximum principal stress and equivalent stress	Cavity nucleation rate	cavity growth rate	rupture lifetime
power law stress index (*a, b*)	3.5~5	3.5~5	3.5~5

3.4. The cavity nucleation and growth at Type IV weldment zone

Literature reveals that Type IV failure is a worldwide problem in power generation systems operating at high temperature; such rupture behavior in the weldment has been seen in low alloys such as: ½CrMoV, 1CrMoV, 2CrMo, 1CrMo and 2.25Cr1Mo or in high alloys such as, P91and P92 [36-37].

At lower stresses, Type IV zone is constrained by the stronger base and weld metal; the models show that damage accumulation is enhanced by multi-axial stress states; however, Smiths [37] suggest the damage on Type IV zone occurs by grain boundary sliding, and damage accumulation is governed by the Von-Mises equivalent stress. The microscopic observation of creep damage on low Cr-Mo alloy steel weldment has been focused on the distribution of the cavitation density number since the typical Type IV failure has been found at grain boundaries [36-38]. Also grain boundary creep cavitation is found in coarse-grained HAZ regions. It also occurs in the intercritical region at the edge of the HAZ, and in the weld, itself.

Cylindrical cross-weld specimens tested at stress range of 80~162MPa and temperature regime from 560℃ to 600℃ [37] indicated that the tested specimens all failed with a low ductility manner in the intercritically transformed region of HAZ which is Type IV failure despite of different heat treatment histories. In all these cases, fracture was a consequence of creep cavity nucleation and growth in the intercritically transformed region of the HAZ which developed into micro/macro-cracking and failure. Intergranunlar creep damage typically observed in the intercritically transformed region of the HAZ. And the advanced micro-crack development is apparent along with large amounts of grain boundary creep cavitation. The fact that eventual failure usually occurred in the fine grain region is apparently because the cavitation there, was so profuse that propagation of a major crack was faster than in the coarse grain region. High level of constraint present with these test-pieces results in creep cavitation and micro-cracking being developed in all regions of HAZ [36-38].

Smith and et al. and Walker [36-37] found that in the cross-weld specimens the creep cavitation occurred across the net section, the numbers of cavities per unit area were quantified as a function of fractions of rupture life. This phenomenon occurs is because of at uni-axial tension specimens the stress concentrated at the net section in the middle part which cause the cavity density increasing. The cavity density and size distribution for various life fractions has been observed by using SEM at 600-640℃, in the specimens of cross weld [36].

Table 6 Experimental data of cavity per unit area, mm², summarized with during rupture time [36].

Time to rupture: T/T_f	0-0.2	0.2-0.4	0.4-0.6	0.6-0.8	0.8-1
Cavity per unit area, *mm²* (16-36MPa, 600, 620,640℃)	800	200-1800	900-1900	1300-1400	2400-2600
Cavity per unit area, *mm²* (48-80MPa, 600, 620,640℃)		400-1000	700-1600	1400-2300	4260
Cavity size (*µm*)	0~0.1	≥0.1	≥0.1	0.1~10	Not addressed

As Table 6 shows that cavity numbers are more pronounced when at the low stress level for life fractions less than about 0.7 T_f [36-37]. The experiments data shown in Table 6 indicate that at the low stress range of 16-36*MPa*, from 0.2-0.7 T_f, the cavity number increasing rapidly from about 200-1300 *mm²*. Similar results has been seen in the specimens tested under 48-80MPa，from 0.2 T_f to 0.7 T_f the cavity density (cavities per unit area, *N, mm²*) increasing dramatically from about 400 to 2000 *mm²*, and then this number rising from 2300 to 4260 *mm²*, at 0.7 T_f to 1 T_f [36-37]. Furthermore, as has been summarised in

Table 6, the cavity growth appears to be only dominant at life fractions close to approximately 70%; this observation illustrates that the cavity growth to larger cavity sizes did not occur until much later in life [36-37]. The average of the cavity size growth becomes noticeable when it grows to approximately the same size as the grain boundary and the micro-crack, for about $10\ \mu m$ at around $0.7\ T_f$ [36 − 37]; these results suggested that there is a process of continuous nucleation and rapid growth to a stable cavity area of about $2\mu m^2$ at low stresses and low life fractions.

The overall aim to analyse the experimental review was to obtain a better scientific understanding of the results that leads to Type IV cavity accumulation and failure in low Cr-Mo alloy steel weld [36-37, 39]. At low stress more cavities are presented at low life fractions ($0.5\ \boldsymbol{T_f}$) than at high stress. For majority of the life of the specimens the peak cavity area was about $2\boldsymbol{\mu m^2}$ [36-37]. Studies of the cavities using SEM did not reveal a large population of small sub-micron cavities. It appears that the growth from nucleation size to an optically visible size was rapid [36-37]. This would be expected if high local (grain boundary) stress concentrations were present at the nucleation site.

4. Creep Rupture Criterion under uni-axial State

4.1. Summary of the existing creep rupture criterion

Table 7 summarizes the different creep rupture criteria which have been applied in creep damage constitutive equations for low alloy; nevertheless, the majority of these creep rupture criteria do not necessarily have good physical meanings reflecting the real creep rupture and rupture mechanism [40]. However, with the results summarized in the paper in terms of cavity nucleation, growth and coalesce, illustrating that the percentage of boundary area fraction may suitable for the creep rupture criterion under uni-axial stress state, at low stress level due to the creep rupture mechanism is suggested as continuous cavitation nucleation and constrained cavity growth mechanism, which has dominant influence on the accumulation of the damage leads to the final rupture behavior.

Table 7 Summery of existing failure criterion for low Cr-Mo alloy creep damage constitutive equations under uni-axial stress [40-50].

Creep models used for low Cr-Mo alloy	Originated from year	Failure criterion
Kachanov [41]	1958	Critical damage $D = 1$
KR (Kachanov Robatnov) [42]	1969	Critical damage ω_c
Lemaitre [43]	1985	Critical damage D_c
Lai [44]	1989	Critical reduction in load-bearing area=A (addressed as 63%)
Piques [45]	1989	$f =$ porosity
KRH (Kachanov–Robatnov-Hayhurst) [46]	1995	Critical damage ω_c
Dyson and McLean [47]	2000	Critical strain at failure $\varepsilon_f = 5\%$
Qiang Xu [4]	2000	Critical damage ω_c
Michel [48]	2004	limit load $\left\|\vec{P}_L(\sigma_0)\right\|$
Lmaitre and Desmorat [49]	2004	Critical damage D_c
Pétry and Lindet [50]	2009	$t_R = Min\{(\varepsilon = 10\%), t(D = D_c)\}$
Whittaker and Wilshire [51]	2012	Limited activity energy: Q_C^*

4.2. Creep rupture criterion--grain boundary area fraction

It is recognized that the presence of grain boundary creep cavities reduces the tensile load bearing cross section area of the specimens; furthermore, large amounts of cavitation damage on grain boundary may introduce plastic instability. In other cases, in particular in the overheated Cr-Mo steels studied by Cane [27-28], the cavity density saturates at some fraction of the lifetime with a saturation value, which increases with stress as $\boldsymbol{N_{sat}} \propto \boldsymbol{\sigma^{1.3}}$. As has been stated that the largest creep density was about $40,000mm^2$ [36-37], and the average grain size is about $5\boldsymbol{\mu m}$ therefore, the largest fraction of cavited grain boundaries in the Type IV narrows zone was about 1 % [36]. In type 304 stainless steel, the cavity density also tends to saturate to a stress-dependent

maximum value [36]. This actual creep damage failure mechanism should be considered as one of the failure criteria in the constitutive modeling work.

5. Result and Discussion

Based on the review of experimental data and the microstructure observation under varying stress ranges, summary of the analysis on quantitative of literatures experimental shows the following conclusions

1) the rupture behavior at low stress level is of intergranular brittle manner;
2) the relationship between the $\dot{\varepsilon}$ and σ is approximately linear behavior at low stress level;
   This relationship indicate that the cavity growth contributes less to the increase of creep strain during the tertiary stage , in comparison that of power law regime.
3) the cavity normally starts nucleation at about 0.2 of the rupture lifetime and its density continuous to grow till about 0.7 of the rupture lifetime;
4) the cavity growth is constrained diffusive mechanism which has been observed from 0.7 of the rupture lifetime;
5) the stress level has great influence on the cavity nucleation rate;
6) cavity size growth had a relatively minor inflation on the overall failure time.

The new set of creep damage constitutive equation to be developed should satisfy the following requirements and should be able to:

(1) represent the transition between lower-shelf intergranular rupture and upper-shelf ductile-transgruanlar rupture as a function of temperature, strain rate, and stress;
(2) depict the mechanistic relationship between minimum stress rate and applied stress, such as equation 2:

$$log\dot{\varepsilon}_{min} \propto n * log\sigma$$

(3) express the mechanistic relationship between applied stress versus time to rupture, such as suggested by Equation 2:

$$T_f \propto \frac{1}{\sigma}$$

(4) reflect the dominated deformation and rupture mechanism should be continuous cavity nucleation and constrained diffusion cavity growth under low stress level, $0.2 - 0.4\ \sigma_Y$;
(5) show, under lower stresses, the uni-axial rupture criterion is amalgamated with the fraction area of cavity on the grain boundaries;
(6) reflect the cavity nucleation and growth rate is strongly dependent upon the maximum principal stress, under low stress, such as suggested by Equation 3 and 4;

$$\dot{N} = \sigma_1^n$$
$$\dot{R} = \sigma_1^m$$

(7) reflect the cavity nucleation and growth rate is strongly dependent upon both of the maximum principal stress and the equivalent stress, under high level, such as suggested by Equation 6 and 7;

$$\dot{N} = \sigma_1^a \sigma_e^b$$
$$\dot{R} = \sigma_1^a \sigma_e^b$$

The most important part in the cavity nucleation and growth rate model is the exponential factor, which makes the nucleation rate a very sharply increasing function of the stress σ. The rupture lifetime could be predicted from knowledge of the nucleation rate determined under uni-axial tensile.

6. Conclusion

A critical review of the stress level influence on large quantities of experiments, in terms of cavitation development, creep strain rate and creep rupture lifetime, indicating that the creep damage evolution turns to be a brittle manner at low stress level; thus, the creep rupture criterion at low stress level should take the cavity development grain boundary fracture into account. Further work will focus on 1) to develop the cavitation kinetic equation, and cavity growth equation, and 2) to design the coupling between the micro cavitation and macro creep deformation and rupture.

7. Reference

1. NIMS creep data sheet, National Institute for Materials Sciences [Online], 3B, 1986, http://smds.nims.go.jp/cgi-bin/MSDS/factOpen/directv8_en.cgi?key=52.

2. Holdsworth S.R. and Merckling G., Developments in the Assessment of Creep-Rupture Properties [Online], ECCC, 2012, http://www.ommi.co.uk/etd/eccc/advancedcreep/SRHGMpap1.pdf.

3. Nuclear Research, Nuclear Research Index Section A [Online], 2010, Structural Integrity, http://www.hse.gov.uk/nuclear/nri-topics/2012/section-a.pdf.

4. Xu, Q. Development of constitutive equations for creep damage behavior under multi-axial states of stress. in: Advances in Mechanical Behavior, Plasticity and Damage, France, Nov. 7-9, 2000; 1375-1382.

5. Xu Q., Wright M. and Xu Q.H. The development and validation of multi-axial creep damage constitutive equations for P91. in: ICAC 11: The 17th International Conference on Automation and Computing, Huddersfield, UK, Sep. 10, 2011.

6. Xu Q.H., Xu Q., Pang Y. and Short M. Current state of developing creep damage constitutive equation for 0.5Cr0.5Mo0.25V ferritic steel. In: The 2nd International Conference on Machinery, Materials Science and Engineering Applications, Wuhan, China, June 16-17, 2012.

7. Hosseini E., Holdsworth S.R., Mazza E. Creep constitutive model considerations for high-temperature finite element numerical simulations, The Journal of Strain Analysis for Engineering Design 2012; 47: 341-349.

8. Xu Q.H., Xu Q. and Pang Y. and Short M. Review of creep cavitation and rupture of low Cr alloy and its welement, in: The 3rd International Conference on Machinery, Materials Science and Engineering Applications (MMSE 2013), Wuhan, China, June 22-23, 2013.

9. Xu Q.H. et al. A review of creep deformation and rupture mechanisms of low Cr-Mo alloy for the development of creep damage constitutive equations under lower stress, in: The 10th International Conference on Scientific Computing, Las Vegas, USA, July 22-25, 2013.

10. Xu Q.H., Xu Q., Lu Z. and Barrans S. A review of creep deformation and rupture mechanisms of Cr-Mo alloy for the development of creep damage constitutive equations under lower stress. Journal of Computer and Communication, 2013; 10: 1043-1054 (accepted and to be published).

11. NRIM creep data sheet. National Research Institutive for Metals. 11B (1997).

12. NIMS creep data sheet. National Institute for Materials Sciences, 36B (2003).

13. NIMS creep data sheet. National Institute for Materials Sciences, 3B (1986).

14. Hayhurst, R.J., Mustata, R. and Hayhurst, D.R. Creep constitutive equations for parent, Type IV, R-HAZ, CG-HAZ and weld material in the range 565-640 °C for Cr-Mo-V weldments, International Journal of Pressure Vessels and Piping 2005; 82: 137-144.

15. Dobrzański J. Internal damage processes in low alloy chromium–molybdenum steels during high-temperature creep service. Journal of Materials Processing Technology 2004; 157-158: 297-303

16. Dobrzański J., Sroka M. and Zielinski A. Methodology of classification of internal damage the steels during creep service. Journal of achievements in materials and manufacturing engineering 2006;18: 263-266.

17. Dobrzański J., Zielinski A., and Krzton H. Mechanicam properties and structure of the Cr-Mo-V low-alloyed steel after long-term service in creep condition. Journal of achievements in materials and manufacturing engineering, 2007; 23: 39-42.

18. Dobrzański J., Zielinski, A., and Sroka, M. Microstructure, properties investigations and methodology of the state evaluation of T23 (2.25Cr-0.3Mo-1.6W-V-Nb) steel in boilers application. Journal of Achievements in Materials and Manufacturing Engineering 2009; 32:142-153.

19. Zielinski A. Dobrzański J. and Jozwik K. Assessment of loss in life time of the primary steam pipeline material after long-term service under creep conditions. Journal of achievements in materials and manufacturing engineering, vol. 54, 2012, 67-74.

20. Kawashima F. et al, Micro-macro combined simulation of the damage progress in low-alloy steel welds subject to Type IV creep failure. JSME International Journal 2004; 47: 410-418.

21. Needham N.G. Cavitation and Fracture in Creep Resisting Steels: Final Report, Commission of the European Communities, 1983.

22. Myers M. R., Pilkington R. and Needham N.G. Cavity nucleation and growth in a 1%Cr−0.5%Mo steel. Materials Science and Engineering 1987; 95: 81-91.

23. Longsdale D. and Flewitt P.E.J. The effect of hydrostatic pressure on the uniaxial creep life of a $2\frac{1}{4}$%Cr1% Mo steel. Proc. R. Soc.Lond. 1981; 373A: 491-509.

24. Riedel, H., Fracture at high temperature, Springer-Verlag, 1986.

25. Lonsdale D. and Flewitt P.E. J. Damage Accumulation and Microstructural changes occurring during the creep of a 2.25Cr1Mo steel, Materials Science and Engineering 1979; 39: 217-229.

26. Liaw P.K. and Rao G.V. Creep fracture behavior of $2\,^{1}/_{4}$Cr-1Mo welds from a 31-year-old. Material science and engineering 1991; 131: 187-201.

27. Cane, B. J. Creep fracture in $2\,^{1}/_{4}$%Cr-1%Mo steel. Metal Science 1976; 10: 29-34.

28. Bissell, A.M. Cane, B.J., Delong, J.F. In: Proceeding conference asme pressure vessels and piping, Pittsburg, 1988; 1.

29. Chen A., Flewitt P.E.J.and Smith D.J. Microstructural sensitivity of 316H austenitic stainless steel: Residual stress relaxation and grain boundary fracture, Materials Science and Engineering:, 2010; 527(27–28): 7387-7399.

30. Viswanathan R. Life assessment of high temperature components, Material aging and component life extension EPRI CA94304; 49-62

31. Dyson B. F. and McLean D. Metal Science 1977; 11:37-45

32. Evans H. E. Mechanisms of creep rupture. Elsevier applied science publishers, London and New York 1984

33. Parker J.D. and Parsons A.W.J. High temperature deformation and fracture processes in 2.25Cr1Mo-0.5Cr0.5Mo0.25V weldments. International Journals of Pressure Vessels and Piping 1995; 63: 45-54.

34. Parker J.D. Creep behaviour of low alloy steel weldments. International Journals of Pressure Vessels and Piping 1995; 63: 55-62.

35. Parker J.D. and Parsons A.W. The tempering performance of low-alloy steel weldments. International Journals of Pressure Vessels and Piping 1994; 57: 345-352.

36. Walker N.S. Type IV creep cavitation in low alloy ferritic steel weldments, Ph.D. Thesis, University of Bristol, 1997.

37. Smith D.J., Walker N.S. and Kimmins S.T. Type IV creep cavity accumulation and failure in steel welds. International Journal of Pressure Vessels and Piping 2003; 80(9): 617-627.

38. Parker J.D. and Stratford G.C. and Westwood H.J. Effects of heat treatment and test specimen geometry on creep fracture in 1.25Cr-0.5Mo welds, ImechE conference 1996; C494: 351-360.

39. Fujiyama, K. et al. Creep life assessment of 2.25Cr-1Mo piping steel and of its simulated HAZ Mterial, Materials science research international. 1997; 3: 237-243.

40. Hore R.N. and Ghosh. Computer simulation of the high temperature creep behaviour of Cr-Mo steels. Materials Science and Engineering 2011; 528: 6095-6102.

41. Kachanov L.M. Time of the rupture process under creep conditions. TVZ Akad Nauk SSR Otd Tech. Nauk 1985; 8: 26-31.

42. Rabotnov Y.N. Creep Problems in Structural Members Amsterdam. North-Holland, 1969.

43. Lemaitre J. and Chaboche J.L. Mecanique of Materials Solides, Dunod, Paris, Springer Verlag, Berlin, 1985.

44. Lai J.K.L. A simple model for assessing the degradation of creep rupture strength after exposure to high temperatures at low stresses. Materials Science and Engineering A 1989; 111: 81-84.

45. Piques R., Molinie E. and Pineau A. Comparison between two assessment methods for defects in the

creep range. Fatigue and Fracture of Engineering Materials and Structures 1991; 14: 871-885.

46. Hayhurst R.J., Vakili-Tahami F. and Hayhurst D.R., Verification of 3-D parallel CDM software for the analysis of creep failure in the HAZ region of Cr-Mo-V crosswelds, International Journal of Pressure Vessels and Piping 2005; 86: 475-485.

47. Dyson B.F., McLean M. Modeling the effects of damage and microstructural evolution on the creep behavior of engineering alloys, ISIJ Int. 1990; 30: 802-811.

48. Michel B. Formulation of a new intergranular creep damage model for austenitic stainless steels. Nuclear Engineering and Design 2004; 227: 161-174.

49. Lemaitre J. and Desmorat R., Engineering Damage Mechanics: Ductile, Creep, Fatigue and Brittle Failures. Springer, Amsterdam, 2005.

50. Pétry C. and Lindet G. Modelling creep behaviour and failure of 9Cr–0.5Mo–1.8W–VNb steel. International Journal of Pressure Vessels and Piping Volume 2009; 86: 486-494

51. Whittaker M.T. and Wilshire B. Advanced procedures for long-term creep data prediction for 2.25 chromium steels, Metallurgical and Materials Transactions 2013; 44: 136-153

52. Yokobori T. and Jr. A. Difference in the creep and creep crack growth behavior between creep ductile and brittle materials. Engineering Fracture Mechanics 1999; 62: 61-78